Continuous Hourly Observations of Chlorophyll Fluorescence, Turbidity and Irradiance in Massachusetts Bay 2005 – 2020

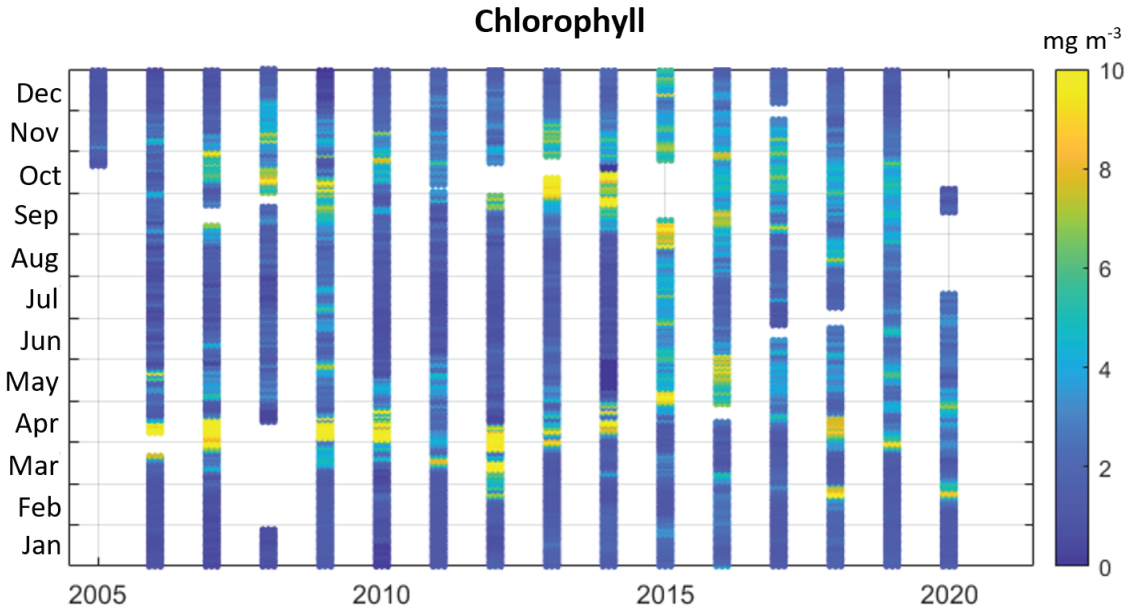

Massachusetts Water Resources Authority
Environmental Quality Department
Report 2021-11

Citation:

Roesler CS. 2021. **Continuous Hourly Observations of Chlorophyll Fluorescence, Turbidity and Irradiance in Massachusetts Bay, 2005 - 2020**. Boston: Massachusetts Water Resources Authority. Report 2021-11. 25 p.

Cover: Hovmöller diagram of chlorophyll concentration.

Environmental Quality Department reports can be downloaded from http://www.mwra.com/harbor/enquad/trlist.html.

Continuous hourly observations of chlorophyll fluorescence, turbidity and irradiance in Massachusetts Bay, 2005 - 2020

Principal Investigator:	Dr. Collin Roesler
Institution:	Bowdoin College Department of Earth and Oceanographic Science
Address:	6800 College Station Brunswick, ME 04011
Phone:	207-725-3842
Email:	croesler@bowdoin.edu

Period of Performance:	1 July 2020 - 30 June 2021

SUMMARY

Since late 2000, the Massachusetts Water Resources Authority (MWRA) has discharged treated wastewater from its Deer Island Treatment Plant in Boston into Massachusetts Bay through an outfall 15 km (9 miles) offshore. To help ensure that nutrients in the discharge do not contribute to excess growth of marine algae, or phytoplankton, the MWRA monitoring program surveys Massachusetts Bay phytoplankton conditions from a research vessel approximately monthly by measuring chlorophyll concentration as the indicator of phytoplankton. The results demonstrate that chlorophyll has remained at natural levels, including near the outfall.

To augment its monitoring, in particular the frequency at which chlorophyll is measured, MWRA since 2005 has contracted with Bowdoin College researchers to operate sensors on a buoy moored off Cape Ann in northeastern Massachusetts Bay. The sensors make continuous hourly measurements of phytoplankton chlorophyll and turbidity, which is a measure of water cloudiness due to suspended particles such as sediments and bacteria. University of Maine maintains the buoy, which collects additional observations, and reports the results in real time online (www.neracoos.org) with support from the Northeast Regional Association of Coastal Ocean Observing Systems and MWRA.

The sensor suite consists of chlorophyll fluorometers, which measure the red light emitted (fluoresced) by phytoplankton chlorophyll in response to a blue or green light flash. As of 2016, Bowdoin has maintained two fluorometers that provide both redundancy and additional colors of light to stimulate fluorescence. Redundancy reduces measurement uncertainty and provides some insurance against instrument failure. Additional colors help identify multiple types of phytoplankton. An irradiance sensor measuring above-water solar conditions is used to reduce uncertainty in the fluorescence measurements. Bowdoin configures and calibrates the sensors, works with University of Maine to deploy and recover them at sea, arranges manufacturer repair and maintenance, and interprets results in the context of oceanographic conditions.

Sixteen years of observations reveal a recurring seasonal pattern with spring and fall increases in chlorophyll due to phytoplankton blooms; the timing, duration, and intensity of blooms vary due to changes in environmental conditions (e.g., sunlight; temperature; density layering, called stratification). Turbidity, on the other hand, has been relatively constant, suggesting that other suspended biological particles, such as bacteria, have changed relatively little. **Conditions during 2019-2020 were typical of other years and did not indicate unusual water quality.**

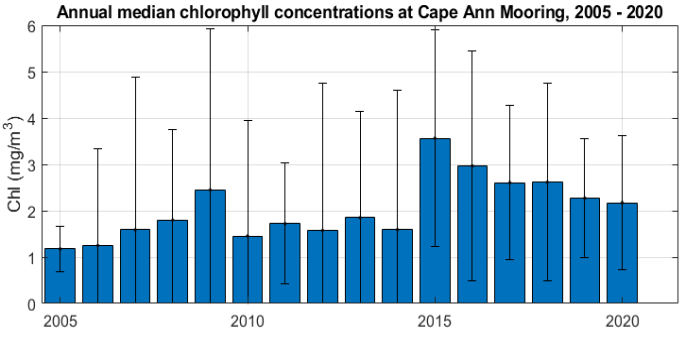

Annual median chlorophyll (blue bars, with standard deviation black lines) exhibits long-term natural variability.

Results also suggest the spring bloom is occurring earlier and lasting longer, and the fall bloom is lasting slightly longer with a decreasing peak height. These variations are most likely regional and due to fluctuating temperature and salinity stratification.

Introduction

This report describes work and results from the 2019-2020 deployment A0142 of MWRA's continuous biological monitoring in Massachusetts Bay, performed by Bowdoin College researchers. The program focus is real-time monitoring of water quality conditions, with emphasis on marine algae (phytoplankton) through chlorophyll measurements, to improve MWRA's ability to detect changes and respond if necessary. MWRA's Ambient Monitoring Plan, attached to its National Pollutant Discharge Elimination System permit to release treated effluent from the Deer Island Wastewater Treatment Plant into Massachusetts Bay, requires this monitoring.

The program consists of bio-optical observations made at a depth of 3 m on the moored buoy off Cape Ann (Figure 1) operated by University of Maine with support from the Northeast Regional Association of Coastal and Ocean Observing Systems (NERACOOS) and MWRA, referred to as Buoy A01 or Mooring A01. When founded in 2005 it comprised a two-channel sensor measuring chlorophyll fluorescence and turbidity. Chlorophyll fluorescence, the red light emitted by phytoplankton in response to their absorption of light, is an indicator of their concentration in seawater. Turbidity is a measure of cloudiness due to suspended particles. It is used to monitor for the presence of other biological particles such as bacteria that might be responding directly to increased nutrient loads. Observations began on October 22, 2005, and there now are approximately sixteen years of hourly observations. In 2016 Bowdoin began also measuring above-water irradiance and multi-channel chlorophyll fluorescence, beginning with deployment A0136 (deployments are numbered sequentially, A0136, A0137, 0138, etc.).

Figure 1. Bowdoin sensors are deployed on Buoy A01 operated by UMaine for the Northeast Regional Association for Coastal and Ocean Observing Systems (NERACOOS). For reference, Boston, the MWRA outfall tunnel extending offshore from its Deer Island Treatment Plant, the outfall diffuser, Cape Ann, and Cape Cod are also annotated.

The focus of this report is the incremental addition of the November 2019 to October 2020 deployment of A0142 to the dataset. The quality assurance and analysis methods are described, and bio-optical interpretations of resulting dataset are given.

Sensors

The WETLabs ECO FLNTU two-channel sensor is the standard bio-optical device that researchers have deployed on the mooring since 2005 (e.g. Roesler 2016). In order to provide continuous observations with no gaps between deployments, we dedicate two such sensors to the program and swap them on/off the mooring at the start of each deployment, so at all times one is in the field and the other is on shore. The WETLabs factory services and calibrates each of the two FLNTU sensors when it is on shore in between its deployments in the field. On the mooring the FLNTU sensor is integrated into a WETLabs DH4 data handler that provides power to the sensor, controls sampling, archives the raw observations of each hourly burst sampling, and provides hourly mean values to a Campbell data controller (Table 1). The controller incorporates the optical observations, together with those from all other buoy sensors, into a real-time data stream and sends it via cell phone modem or satellite communications to UMaine. There, the data stream is parsed, calibrations are applied to it, and it is made available at the online data portal http://gyre.umeoce.maine.edu/data/gomoos/buoy/html/A01.html and sent to NERACOOS, which also presents it online in real time at their website www.neracoos.org.

Table 1. Components of the optical sensing package on the buoy.

INSTRUMENT	PURPOSE
WETLabs ECO **FLNTU**	Optical sensor, measures chlorophyll fluorescence (470 nm excitation) and turbidity, at 3 m depth.
WETLabs ECO **FL3-WB** ("F3WB")	Optical sensor, measures chlorophyll fluorescence (3 excitation wavelengths), at 3 m depth.
Satlantic OC507-ICSA	Optical sensor, measures solar irradiance; mounted on the buoy tower.
WETLabs DH4	Data logger, collects and stores data from optical sensors; computes mean FLNTU data; transmits means to Campbell Data Logger, which transmits it in real time to the University of Maine where it is relayed to NERACOOS and posted online.

Additional bio-optical sensors are deployed, in a stand-alone configuration integrated into the same DH4, but their data are not transmitted in real time due to limitations on the Campbell software. There is a significant time lag for processing of these additional data, as instruments must be recovered from the mooring, transported to Bowdoin, cleaned, downloaded and post-processed. However, it is then possible to recover the full data set from the FLNTU, comprised

of a one-minute sample burst each hour, with each burst consisting of approximately 60 readings. These values are analyzed to ensure the mean value reported in real time is a robust estimate of the sample burst observations, by comparison to their median and standard deviation.

In addition to the FLNTU, optical sensors include, first, a multi-channel fluorometer which is a custom made WETLabs ECO Triplet sensor FL3-WB ("F3WB" in tables and figures) that consists of 3 excitation channels (435nm, 470nm, 532nm) and one emission channel (695nm) to detect chlorophyll fluorescence stimulated by different accessory pigments in phytoplankton that absorb in the three wavelength bands (Figure 2). This sensor has been used to detect changes in phytoplankton community composition in Maine Lakes (Proctor and Roesler 2010), the Arabian Sea (Thibodeau et al. 2014), the western Mediterranean Sea (Roesler et al. 2017b) and in eastern Casco Bay (http://bowdoin.loboviz.com). Phytoplankton community composition is the relative abundance of different types of phytoplankton present together in seawater, which varies naturally from location to location and temporally, and is an important aspect of water quality and ecological conditions. Chlorophyll concentration is a useful measure of phytoplankton concentration but does not capture phytoplankton community composition.

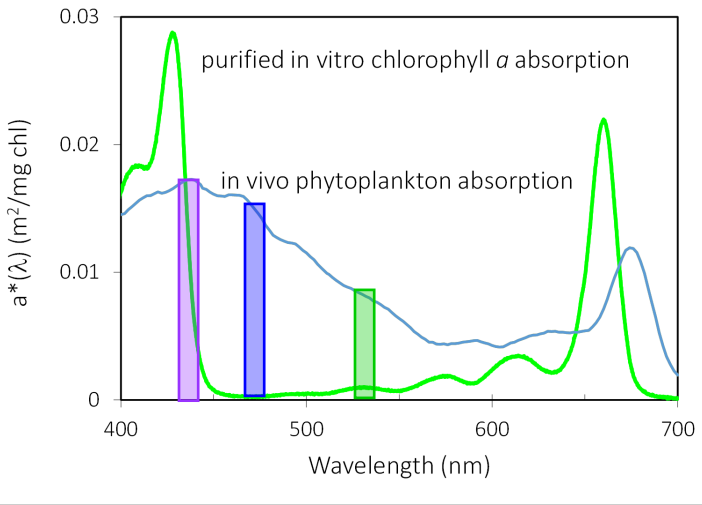

Figure 2. Chlorophyll mass-specific absorption spectra for a purified extract of chlorophyll *a* in 90% acetone (green line) and for absorption by phytoplankton *in vivo* (grey line). The bars indicate the 435 nm (purple), 470 nm (blue), and 532 nm (green) excitation bands for the F3WB chlorophyll sensor. The FLNTU chlorophyll sensor also employs the 470 nm excitation.

Second, a Satlantic OC507-ICSA seven-channel irradiance sensor is deployed on top of the mooring and connected to the subsurface DH4 via a long cable through the well of the float. This sensor is factory calibrated and provides hourly estimates of incident downwelling irradiance E_D ($\mu W\ cm^{-2}$) for seven wavelength bands.

Instrument Calibration. Recent work has concluded that the factory calibrations of the WETLabs ECO model chlorophyll fluorometers are biased by a factor of 2 (Roesler et al. 2017a). For this reason, the laboratory calibration for the chlorophyll fluorometer has always been implemented for sensors on Buoy A01, instead of factory calibrations. All fluorometers are calibrated in the lab prior to deployment using ten dilutions of a monospecific culture of the diatom *Thalassiosira pseudonana* (Proctor and Roesler 2010). The culture is grown in nutrient

replete L1 media at an irradiance that maximizes growth rates (i.e. ~50 W m^{-2}) and minimizes pigment packaging due to low light acclimation. The culture is harvested during exponential growth with maximal extracted chlorophyll concentrations between 20 mg m^{-3} and 50 mg m^{-3} (Figure 3).

This approach to calibration provides a transfer function between sensors and between a single sensor over time, accounting for variations in sensor gain, and also provides conversion of the signal from digital counts (millivolts) to biogeochemical units (mg m^{-3}). Because the excitation wavelength (470 nm) does not directly stimulate chlorophyll fluorescence, it is not possible to calibrate with a standard dilution of purified pigment (blue bar in Figure 2). *In vivo* fluorometers take advantage of the energy transference between accessory pigments in the light harvesting complexes to chlorophyll *a* by stimulating accessory pigment absorption at 470 nm. While the fluorescence yield (fluorescence per extracted chlorophyll) can vary up to 10-fold between species (Figure 3), as a function of environmental acclimation, growth phase, and non-photochemical quenching, each of these sources of variability can be assessed on long-term time scales of observations and thus the impacts can be minimized or exploited for further information (Roesler and Barnard 2013). The selection of the species *Thalassiosira pseudonana* was based upon it ease of culturing, its robust and invariant fluorescence yield from year-to-year calibrations and that it represents the median fluorescence yield value for the range of thirteen diverse, but ubiquitous, species studied by Proctor and Roesler (2010). Global analyses of the fluorescence yield obtained from field comparisons of *in situ* fluorescence and paired

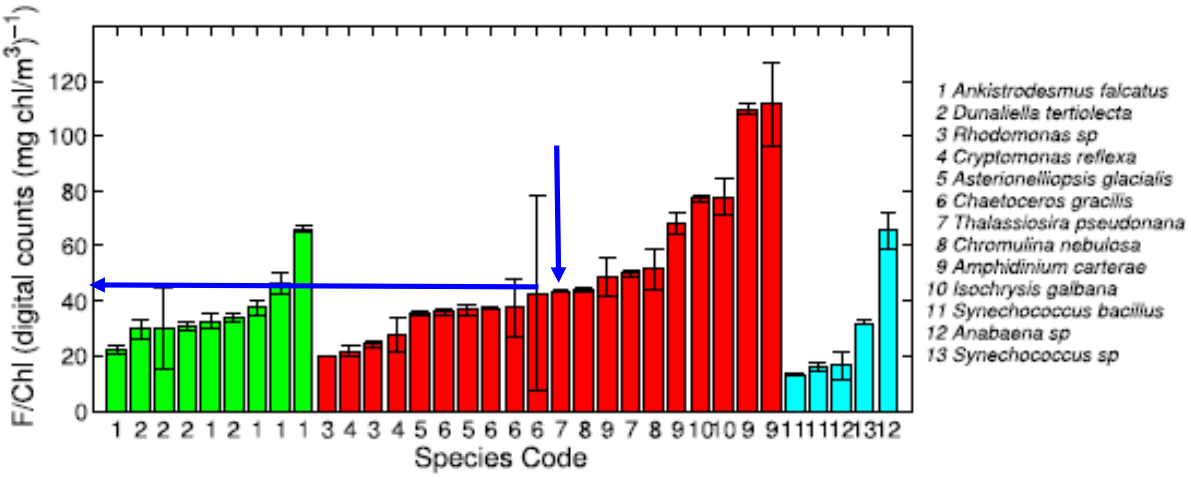

Figure 3. Fluorescence yield (observed fluorescence per extracted chlorophyll concentration) measured with an *in situ* chlorophyll fluorometer under 470 nm excitation for thirteen species (number codes in key) cultured under a range of growth irradiances and in different growth phases. Errorbars represent the variation in derived yield values obtained from dilution series calibration experiments conducted for each culture and experimental condition. Bar colors indicate pigment-based taxonomic grouping into the green, red, and cyano lineages. Blue arrows show the yield values for *Thallasiosira pseudonana* cultured under the environmental conditions described in the text.

HPLC-measured chlorophyll concentration demonstrated that this median response was representative of global patterns (Roesler et al., 2017a).

Detailed explanation of the 7-step post-processing of the real-time data for quality control

As explained in detail in prior reports (e.g., Roesler 2020), a series of processing steps are necessary to maintain the high quality of the dataset.

Step 1. Quality assurance on times recorded by the irradiance sensor.

Step 2 (added this year). Calibration comparison and correction between sensors.

Step 3. Correction for sensor drift.

Step 4. Removal of biofouled data.

Step 5. Identification, flagging, and correction of chlorophyll fluorescence observations impacted by non-photochemical quenching (NPQ).

Step 6. Removal of single value outliers (SVOs).

Step 7. Identify values below minimum detection levels.

Details and examples for all steps other than #2 can be found in Roesler (2020).

Specific issues of data processing for deployment A0142 are described below.

There were instances of gaps in A0142 data reported from the realtime portal. On March 29, 2020, the 1-m deep conductivity-temperature-depth (CTD) sensor stopped reporting. The realtime data stream from optics package was caught in this malfunction because of a dependence in the application of calibration coefficients. In the early years, optical sensors exhibited a small temperature dependence that has since been corrected by the factory. The schema for applying the calibration had not been removed (although the scaling factor was 1.0, so there was no correction, but the step was still 'dependent' upon temperature values from the CTD). Upon recovery of A0142, the data from March 29, 2020 to June 14, 2020 was retrieved from the DH4. There were data from June 14, 2020 to July 20, 2020, but significant rows of data (realizations) were garbled such that automated processing was not possible. The data were QA/QC'ed by hand to retrieve sufficient observations in each hourly burst sample to compute mean values with coefficient of variation values comparable to those outside the garbled time interval. There were not data stored on the DH4 past July 20, 2020. On September 18, 2020, UMaine performed a reset on the Campbell communication ports in hopes of resetting the CTD. The optical sensors resumed relaying data to the DH4, which computed mean values to the Campbell. However, the DH4 did not archive the raw values. The communication problem that caused data loss for surface optics and hydrographic packages during the mid-July to mid-September period is not yet fully understood. It occurred late in a deployment that was extended longer than normal due to COVID-related schedule disruptions.

It should also be noted, however, that a similar issue occurred in the subsequent deployment (A0143), to be included in a future report.

The result for A0142 is that the optical data sets for the FLNTU, FL3-WB, and OCR507 are complete from November 26, 2019 to July 20, 2020, and then from September 18, 2020 to October 4, 2020. The data recovered in the unarchived DH4 data stream is only mean values and the 532 nm excitation channel of the FL3-WB is not reported.

Step 1. Quality assurance on times recorded by the irradiance sensor.

While the FLNTU fluorometer/turbidity and the FL3-WB fluorometer sensors record timestamps aligned with those of the buoy real time data stream, the irradiance sensor, as recorded by the DH4, does not. Occasionally there are some variations in the timing of the irradiance sensor samples, as well as some jumbled transmitted data packets. What was learned during the A0142 deployment, amid the challenges of missing data, is that the realtime DH4 data stream captured by UMaine necessarily contains the time vector for each hourly sampling. So, while it doesn't contain the raw values that comprise the mean, it does remove the uncertainty in the time vector for the irradiance sensor. This discovery means that there will be no uncertainty in the time vector in the future as the archived data can be assigned the time vector from the realtime data array. A disadvantage is that the UMaine time series only records mean values, while the DH4 archive contains the raw burst sampling which enables computing median and standard deviation values for each hour. Median values provide more robust estimates of the burst sampling, leading to a reduction in data flagging during intervals with structural biofouling (explained below).

Step 2. Calibration comparison and correction between sensors. Sensors are routinely returned to the factory for calibration, maintenance and repair. Turnaround times have been increasing and during the COVID-19 pandemic, this was not possible as there were no staff on site at the factories to perform these tasks. Wait times now are very high and it will likely take a few years to get to a situation with predictable turnaround times that make annual factory calibrations operational. Sensors continue to be calibrated in-house where and when possible.

For irradiance sensors, we rely on the long time series of observations and models of maximal irradiance at this latitude, such that the overall seasonal patterns in irradiance can be used to scale the sensors on each deployment (Figure 4). A record of the scaling factors on the calibration coefficients is kept and will be re-evaluated once sensors can be returned to the factory for absolute calibrations. Using the expected seasonal pattern in irradiance provides a robust scaling factor that yields both reliable magnitudes and spectral dependence in the irradiance observations, while preserving hourly variations due to clouds.

Chlorophyll fluorometers are routinely calibrated between deployments using a monospecific culture and conditions described elsewhere (Roesler 2014). Due to slight variations in LED full width half maximum band width for excitation, small intercalibration differences are observed between sensors with nominally the same excitation/emission channels, e.g., FLNTU

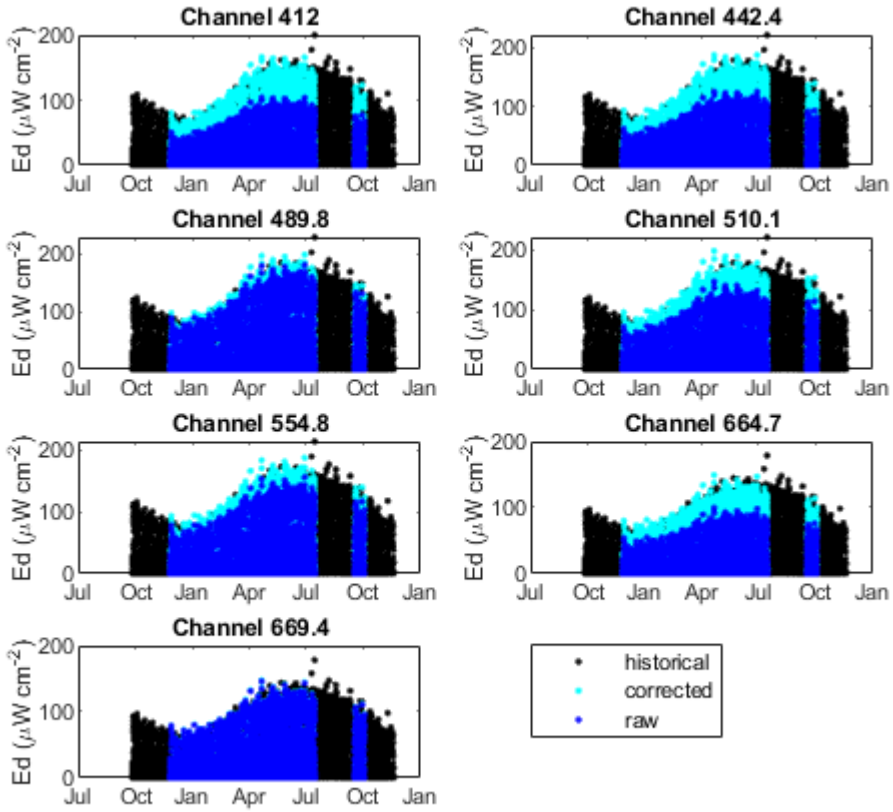

Figure 4. Time series observations of hourly irradiance in each wavelength channel (nm) for historical observations from all years during the date ranges shown (black symbols), raw observations from deployment A0142 (blue), and corrected for intercalibration factors (cyan).

chlorophyll sensor and the FL3-WB 470 nm excitation channel. The response between these two sensors is routinely examined during each deployment; differences in fluorescence responses are typically less than 5%.

For deployment A0142, the comparison between the 470 nm excitation chlorophyll fluorescence on the FLNTU and F3WB shows strong one-to-one covariation (black symbols, Figure 5) for most of the deployment. Selecting just the observations that were not flagged for biofouling yielded comparable estimates of chlorophyll concentration. A type II regression between those data points indicated a slope of 1.05 (cv of 0.3%) and an intercept not statistically different from zero. This difference is within the calibration uncertainty and thus no slope correction was applied.

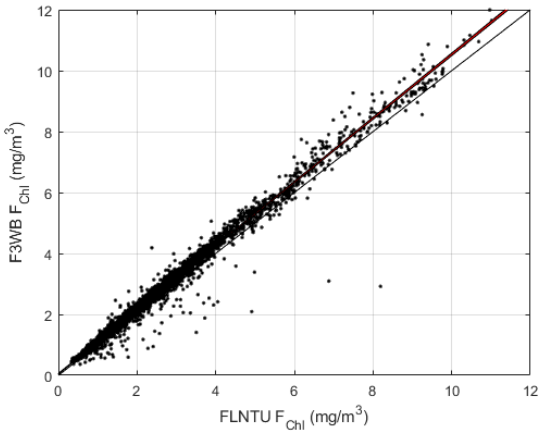

Figure 5. Relationship between simultaneous chlorophyll concentration estimates measured with the F3WB channel 2 fluorometer and the FLNTU fluorometer for all A0142 observations (black symbols). One-to-one and least-squares regressions lines shown (light and bold, respectively).

Step 3. Correction for sensor drift. Offsets can occur between recovery/deployment of sensors. The offsets are evaluated by post recovery calibration or by identification of offset relative to prior and subsequent deployments. It can be challenging to identify offsets in the FLNTU sensor signals due to the intense biofouling that can occur at the end of deployments. The shuttered F3WB sensors are much less vulnerable to biofouling and typically exhibit no or negligible offsets between deployments for all three fluorescence channels. Examining the offsets between deployments provides information on sensor drift in the previous deployment or discrepancies in calibration between deployments. No apparent offsets were observed between any of the sensor channels between deployments 141 and 142 (Figure 6).

Step 4. Removal of biofouled data. Biofouling manifests as a logarithmic signal increase leading to out-of-standard range or to saturating values. Biofouling takes two forms, a smooth signal increase associated with biofilm growth or an extreme hour-to-hour variability due to structural growth such as seaweed on the sensor or frame that contaminate both the fluorescence and turbidity signals as they waft into the optical sensing volume. Biofouling flags are applied separately as either biofilm or structural based upon the pattern of anomalous observations. Mild biofouling effects can be corrected, otherwise the data are removed. Deployment A0142 was noteworthy for the lack of biofouling in the sensors (Figure 7). None of the chlorophyll fluorescence observations displayed biofouling, and only 4 days in September reveal amplified observations that might flag as biofouling in the turbidity sensor. However, wind and wave height observations reveal wind speed in excess of 12 m/s (25 mph) and significant wave height in excess of 5 meters (15 feet). For this reason, the turbidity data were not flagged.

Step 5. Identification, flagging, and correction of chlorophyll fluorescence observations impacted by non-photochemical quenching (NPQ). See Step 4 in Roesler (2020). Figure 8A shows results of the NPQ correction for A0142.

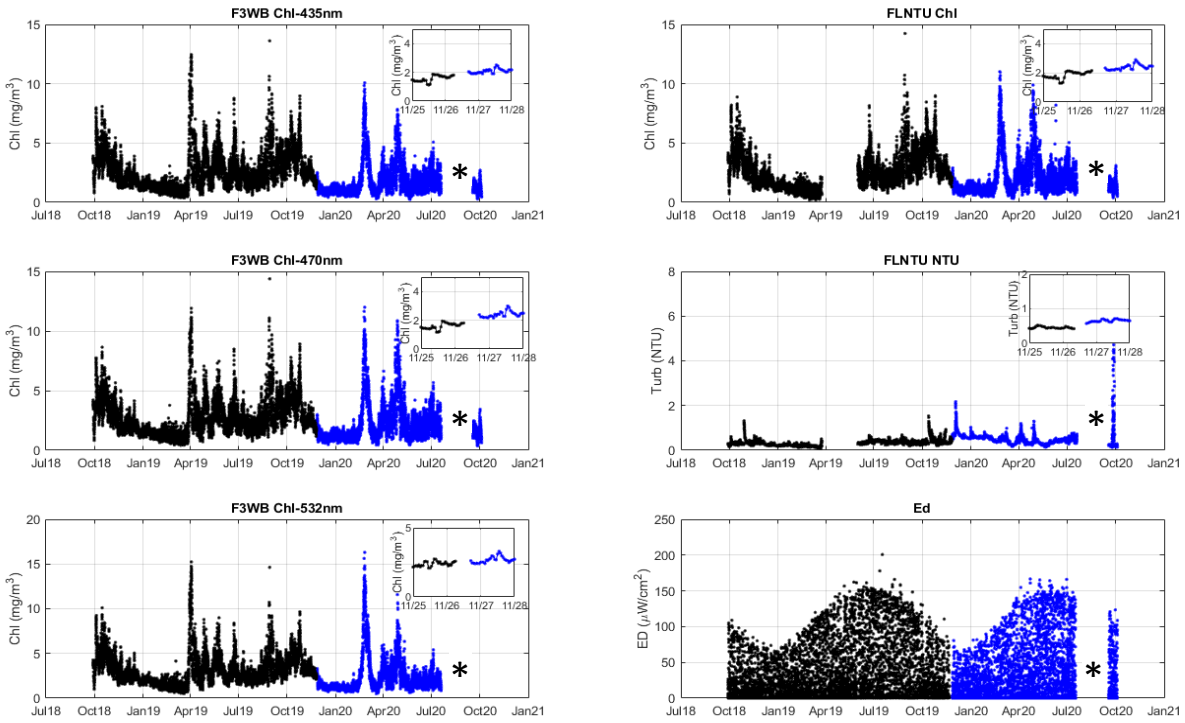

Figure 6. Time series observation of chlorophyll, turbidity, and irradiance for A0140-41 (black) and A0142 (blue) for each deployed sensor. Insets highlight calibration match between end of A0141 and start of A0142. *COVID-related data loss.

Step 6. Removal of single value outliers (SVOs). SVOs are identified as differences between successive consecutive measurements that exceed the coefficient of variation and are in excess of 15 mg/m^3 (chlorophyll) or 3 NTU (turbidity). Single Value Outliers are flagged and removed from the data streams. For deployment A0142, the only SVO values were observed during the 4-day wind and wave event in the turbidity time series. These were initially flagged as outliers following the established SVO criteria; however, as noted above, due to storm conditions it is likely that these data are not outliers so the outlier designation was removed from the final data.

Step 7. Identify values below minimum detection levels. The minimum detection levels (MDLs) of the chlorophyll, turbidity, irradiance and radiance sensors are 0.05 mg/m^3, 0.05 NTU, 0.06 μW m^{-2} and 0.0003 μW m^{-2} sr^{-1}, respectively. Observations below -1*MDL are flagged and removed. Values between -1*MDL and 0, and those between 0 and +1*MDL are independently flagged, for convenience of entering the data in the MWRA database where different value qualifiers are applied to the two ranges. The negative values are not removed because removing negative values within an MDL of zero leads to positive biasing of the observed data (Thompson 1998).

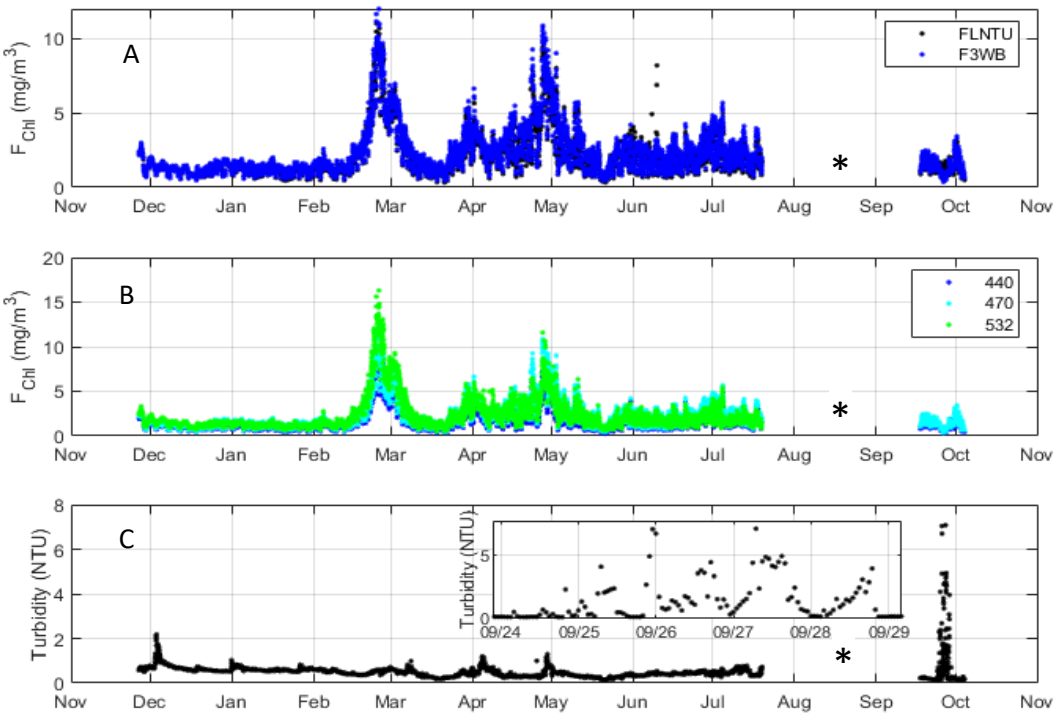

Figure 7. A0142 hourly observations of chlorophyll fluorescence from A. 470 nm excitation chlorophyll fluorescence from the unshuttered FLNTU sensor (black) and shuttered F3WB sensor (blue), B. all channels of F3WB, and C. turbidity sensor. *Inset* Four-day interval of amplified turbidity suspected of biofouling but associated with a high wind and wave event. *COVID-related data loss.

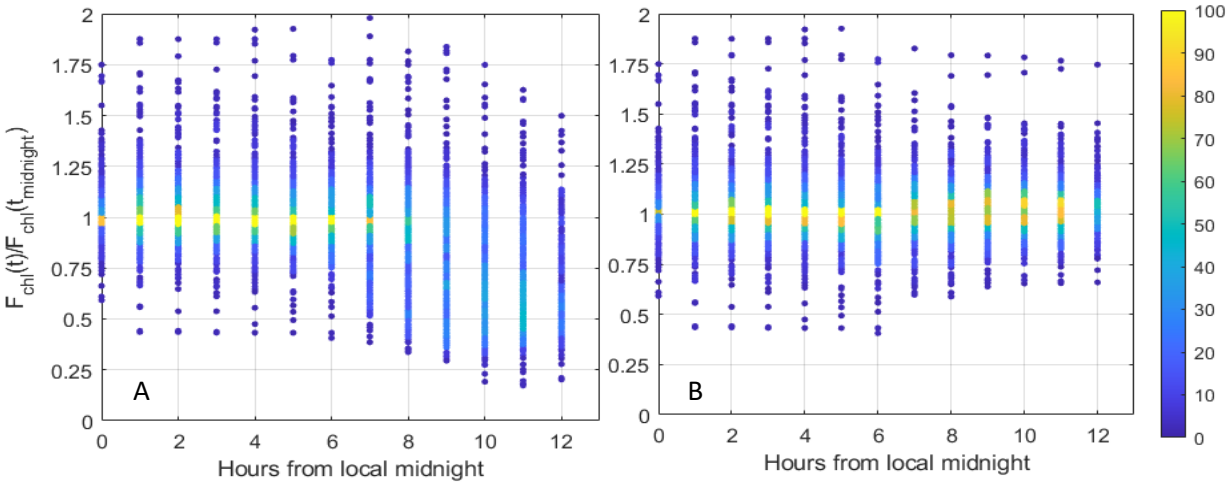

Figure 8. Heatmap (number of observations color-coded) of ratio of hourly (A) raw and (B) NPQ-corrected chlorophyll fluorescence to adjacent midnight fluorescence as a function of hours from local midnight. A ratio of one indicates no NPQ. Scatter indicates sub-diel patchiness in phytoplankton populations.

Data products provided. In order to give a clear sequence of observations, flagging and correction steps, we provide hourly data arrays including each stage of the post-processing. These are also helpful for optimization of correction schemes for biofouling and NPQ.

Separate data files are submitted for:

- the chlorophyll (Chl) and turbidity (NTU) sensors of the FLNTU,
- each channel of the calibrated ECO F3WB chlorophyll fluorometer (F1 through F3),
- the 7-channel irradiance (ED7).

The Appendix provides data string formats:

Table A1 provides the data string for hourly chlorophyll fluorescence data obtained from the ECO FLNTU and FL3-WB sensors.

Table A2 provides the data string format for the hourly turbidity.

Table A3 provides the data string format for the hourly downwelling irradiance and upwelling radiance data files.

Table A4 provides a list of the data file names, descriptions, units and array sizes.

The data arrays provided have the Matlab binary storage “mat” file format.

Results and Discussion

Time series bio-optical observations. The time series bio-optical observations from the FLNTU span 2005 through October 2020 while the observations from the F3WB and irradiance sensors (deployments A0137-A0142) span from June 2017 to October 2020 (Figure 9). **The most recent deployments exhibit lower variability in both chlorophyll and turbidity compared to most previous years.**

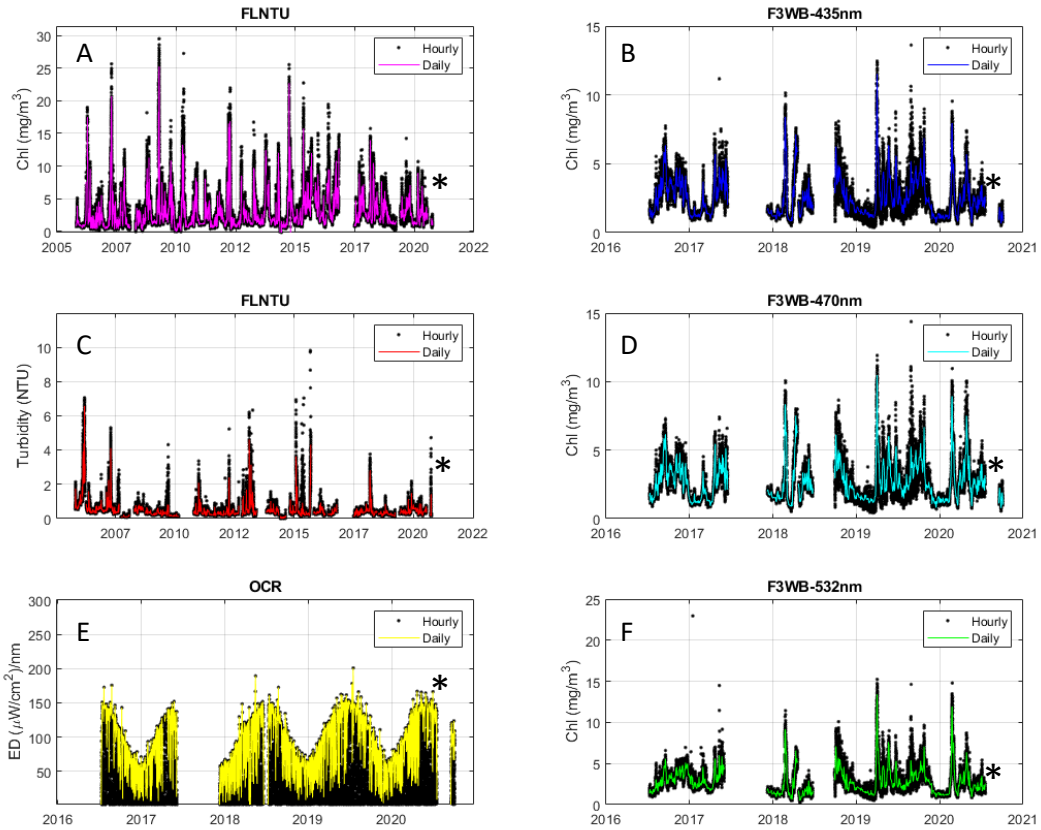

Figure 9. Time series of hourly (black symbols) and daily (colored lines) observed chlorophyll fluorescence (A, B, D, F), turbidity (C), and solar irradiance (E). Daily values represent medians for all but irradiance which is the daily maximal value. *COVID-related data loss.

Long-term annual climatology. The daily climatological values for the bio-optical time series (Figure 10) clearly show that there is a distinct and narrow spring bloom that peaks in early April and a broad fall bloom of slightly lower magnitude that spans September through November. Minimal chlorophyll concentrations are observed during the winter (late December through March) and summer (July). The pattern over the last 4 years of F3WB observations indicates that a spring bloom can occur as early as February and that up to four separate spring blooms can be observed. The fall bloom pattern is much less variable, with a longer duration and a similar magnitude in peak concentration.

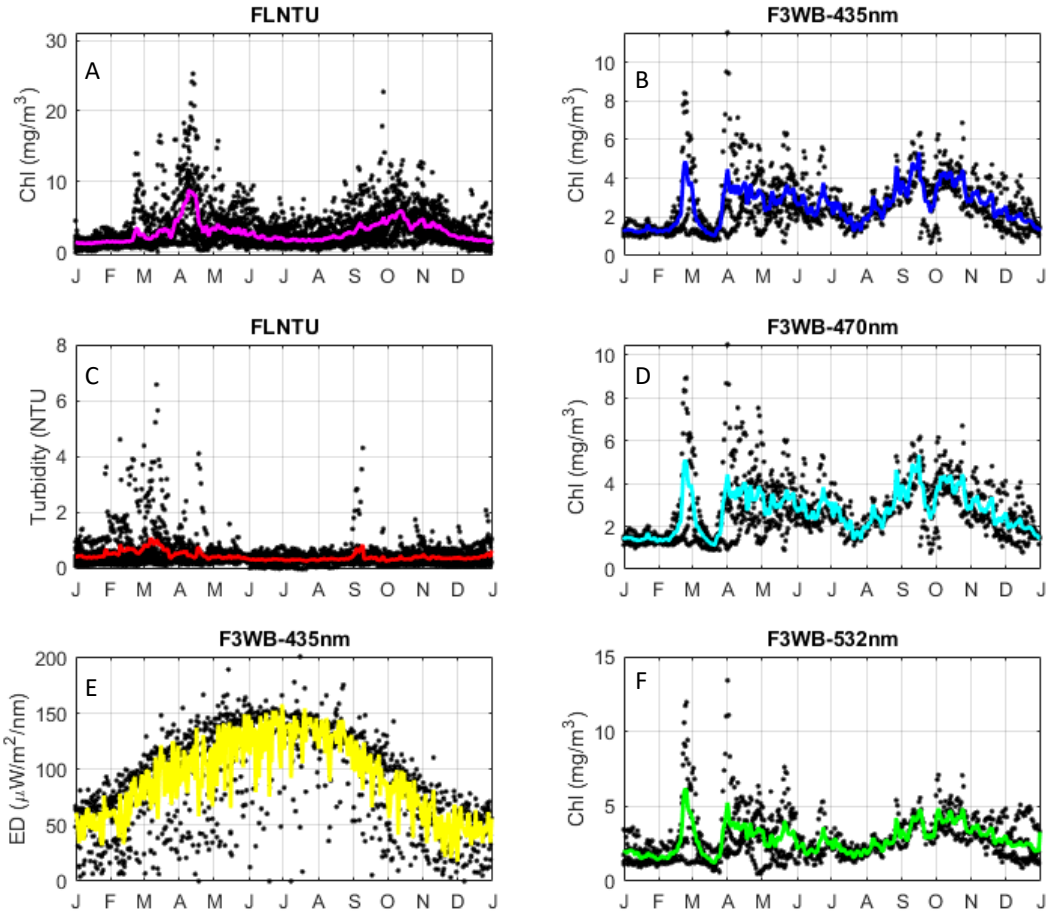

Figure 10. Daily observations (black symbols) and climatological means (colored lines) for the bio-optical time series (Figure 9).

Monthly climatological means for the bio-optical time series are shown in Figure 11. For the 16-year data sets, the spring bloom occurs in April and the fall bloom peaks in October. The magnitude of the spring bloom is slightly smaller than that of the fall bloom and much more variable (Figure 11A). The summer minimum is more variable in magnitude than the winter minimum. The monthly means for the past four years are slightly different from the longer-term monthly patterns (Figure 11 B, D, F) with the peak of the spring bloom occurring in May and both blooms having more extended durations. The seasonal pattern in turbidity is essentially flat through the year (Figure 11C), however, there is substantial variability January through April when winter storms drive events in increased turbidity. September also appears to be a month of higher variability. The monthly pattern in solar irradiance (Figure 11E) reveals peak irradiance in July, minimal in November and December, with March through June exhibiting the most variability. The hourly patterns in irradiance indicate this is consistent with increased cloudiness late spring to early summer compared to the summer and fall months.

The observations during deployment A0142 evidence a spring bloom in April, consistent with the climatology but with much lower values in the fall months, likely due to problems associated with sampling. Turbidity was generally higher than the climatology during winter months and June through July.

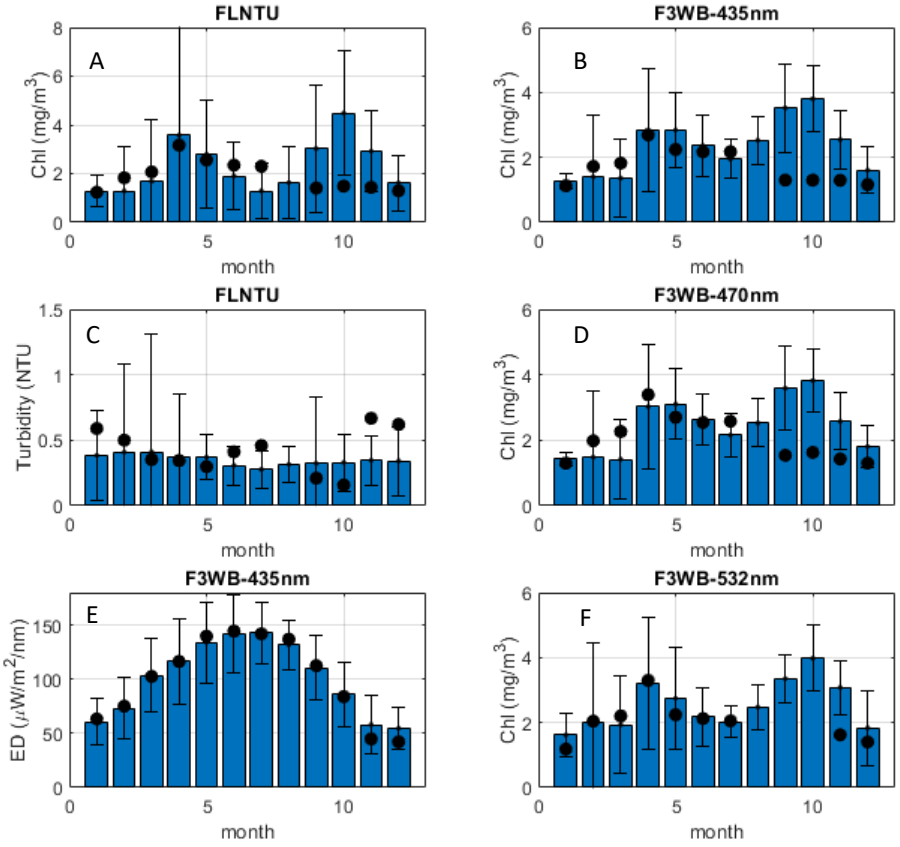

Figure 11. Monthly median (blue bars; all years) values of chlorophyll fluorescence (A, B, D, F), turbidity (C), and solar irradiance (E); error bars indicate standard deviation. Observed monthly median values for A0142 shown as black symbols.

Annual median values of the bio-optical observations reveal a trend of increasing chlorophyll from 2005-2009, an interval of relatively constant annual chlorophyll from 2010-2014, and a highest chlorophyll concentration in 2015, with decreasing values from 2016-2020 (Figure 12A). The annual mean pattern in turbidity exhibits a decrease from 2005-2009 followed by more uniform mean values over the past decade (Figure 12B). Three years (2006, 2013 and 2015) have exhibited the strongest variability. There is not sufficient length of observations to interpret the irradiance or FL3-WB observations.

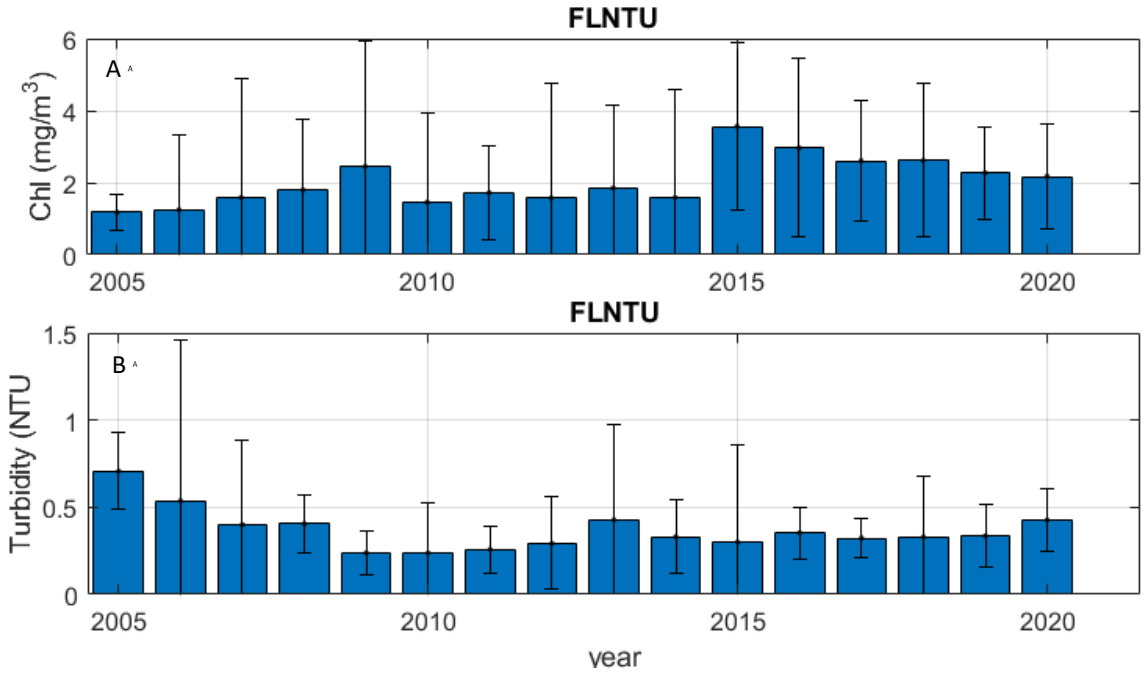

Figure 12. Annual medians of daily values of A. chlorophyll concentration and B. turbidity, error bars represent standard deviations.

The pattern in annual median chlorophyll concentrations can be driven by high peak concentrations during blooms, longer blooms or overall higher sustained concentrations. A Hovmöller diagram (Figure 13) is used to identify which factor may be at play. From 2006 through 2010 a dominant spring bloom occurred in April with a minor secondary bloom in June. In 2011 and 2012 the spring bloom was early by about 2-4 weeks. From 2013 through 2016, the major spring bloom occurred increasingly later in the spring, to approximately late May by 2016. 2018 and 2020 both exhibited a late February bloom, of much higher magnitude than that observed in 2012. Secondary blooms occurred in April and May. The fall blooms have varied from September to November. Since 2017, the magnitude has decreased.

These long-term variations and trends are most likely due to regional changes in temperature and salinity stratification (Thomas et al. 2017).

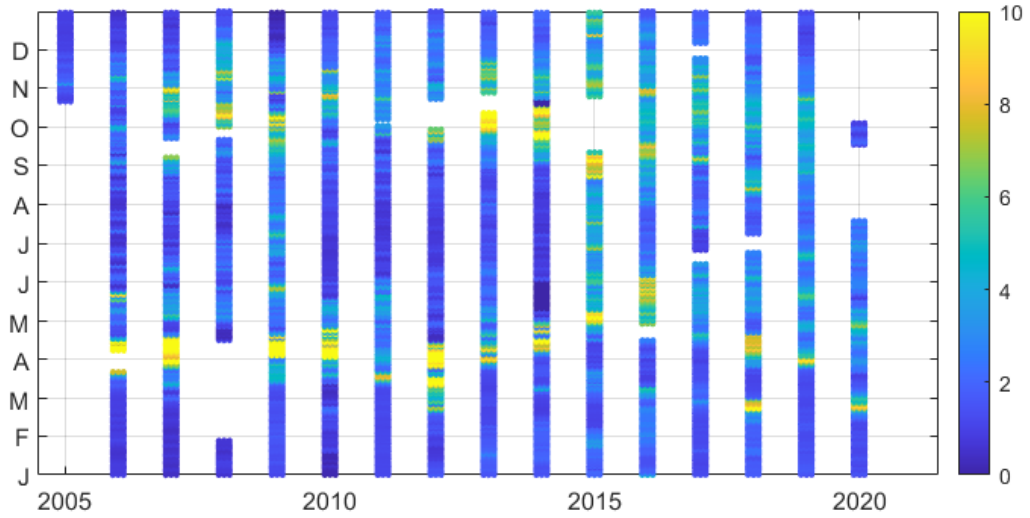

Figure 13. Hovmöller diagram of chlorophyll concentration over the entire bio-optical times series at Buoy A01. Units of colorbar are mg chl/m^3.

Temporal patterns in phytoplankton community composition. The WETLabs FL3-WB, three-excitation single emission chlorophyll fluorometer, yields time series of the intensity of the chlorophyll fluorescence in response to each excitation wavelength that varies as the absorption coefficient at that wavelength varies, and thus as the pigment composition varies (Figure 2). Thus, fluorescence ratios, once corrected for NPQ, are comparable to pigment absorption ratios. The power of the ratios is that it removes the impact of biomass and represents solely pigmentation differences. Raw fluorescence for each channel is calibrated to the diatom *Thalassiosira pseudonana*, thus ratio values of 1.0 indicate diatom domination. Variations from 1.0 indicate variations in pigment composition relative to the diatom signal (Proctor and Roesler, 2010; Thibodeau et al. 2014).

The A0142 F3WB time series is somewhat patchy due to the data gaps. By combining the entire data set there is more representation over the months though not a continuous sequence. That said it is worthwhile to examine the patterns revealed over seasons. Daily median values of F_{470}:F_{440} and F_{532}:F_{440} projected into the ratio space where different regions are inhabited by distinct pigment-based phytoplankton groups (Figure 14).

By way of an example from a region with a complete annual cycle and accompanying pigment composition and taxonomic analysis revealed a pattern of how the fluorescence ratios evolved over the season (Figure 14A) with each season evidencing specific locations in ratio-ratio space. Once pigment analyses, performed by high performance liquid chromatography, are analyzed for phytoplankton community structure, the ratio-ratio space can be distinguished into classification regions and the time evolution of the taxonomy identified. For this example in the Mediterranean Sea (Figure 14B), the winter season (ratio-ratio space centered on 1.4, 2) is

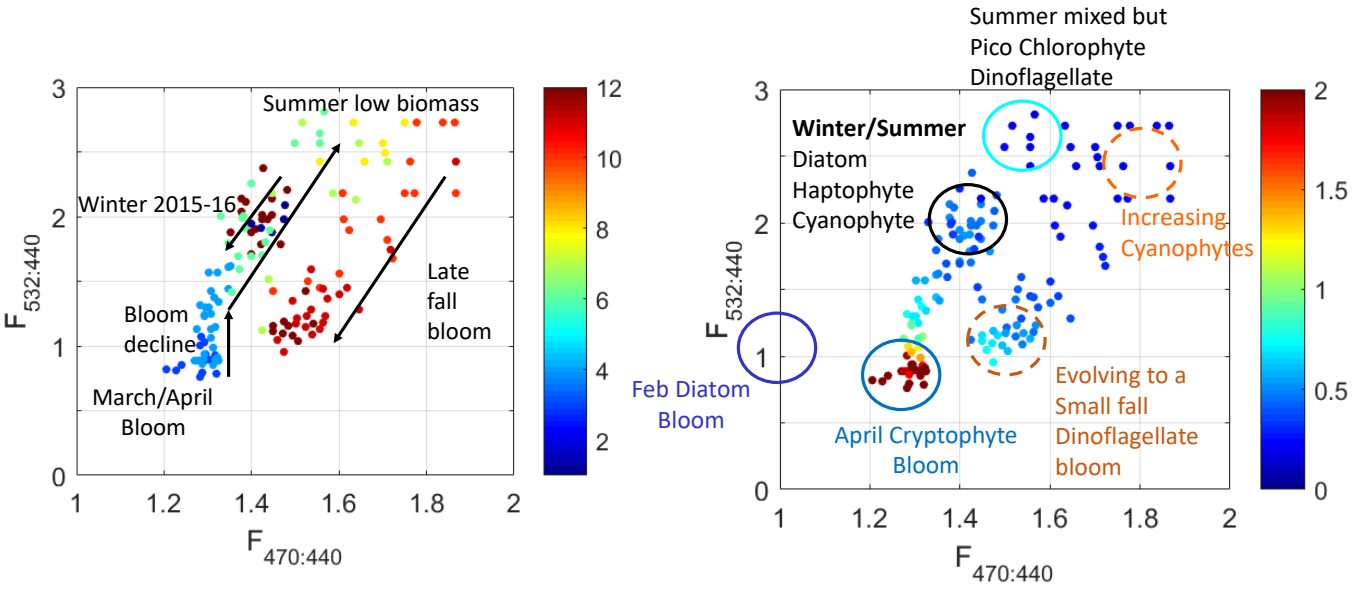

Figure 14. Ratio-ratio representation of the data retrieved from the WETLabs multichannel fluorometer deployed at the Boussole mooring site (Antoine et al. 2008) in the Mediterranean Sea in 2011. A. Symbols color-coded by month, arrow representing the temporal evolution of the observations. B. Data as in A color-coded by chlorophyll concentration to show the location of blooms and seasonal low biomass. Circles indicate the distinct regions for which phytoplankton pigment analyses revealed community composition associated with specific locations in ratio-ratio space. Figures from Roesler et al. (2017b).

dominated by pigments associated with a mix of diatoms, haptophytes and cyanophytes. Through the spring a distinct diatom bloom was observed in the pigments (unfortunately the battery on the fluorometer had died and so the assumption is that it would have projected to

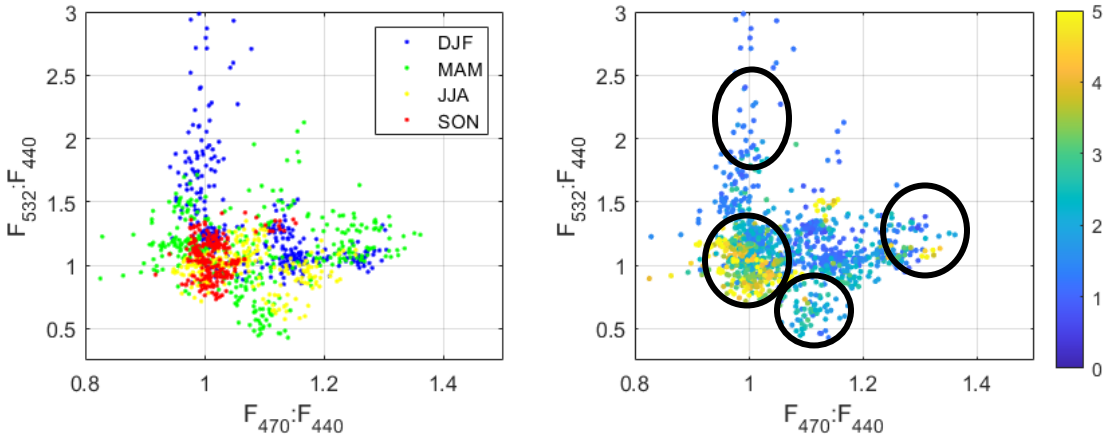

Figure 15. Fluorescence ratio-ratio display of the time series of daily median values of fluorescence measured at mooring A with the WETLabs F3WB multichannel fluorometer. Data points are color-coded by A. season and B. chlorophyll concentration. Circles associated with distinct pigment groups as in Figure 14.

ratio-ratio space (1,1). The diatom bloom evolved into one dominated by cryptophytes (1.2, 1) declining back to a low biomass community similar to the winter community (1.4, 2). By summer the community evolved to very small chlorophytes in the picoplankton size range and small dinoflagellates, followed by a transition to cyanobacteria. There was a small bloom in the fall dominated by dinoflagellates (1.4, 1.2), that transitioned back to the winter population.

Using these results to interpret the ratio-ratio space inhabited by the observations from mooring A, yields a sequence of a distinct fall bloom of diatoms (1, 1), early winter communities of haptophytes (1, 2) evolving to a community of diatoms (1,1) followed by dinoflagellates (1.3, 1.2). Spring and summer transition between diatoms and dinoflagellates with a late summer, early fall population of cryptophytes (1.1, 0.5). If the opportunity becomes available to collect water samples for HPLC pigment analyses and imaging in flow microscopy by Bowdoin, it would be possible to validate the fluorescence fingerprint time series.

References

Carberry, L., C. S. Roesler, and S. L. Drapeau. 2019. Correcting in situ chlorophyll fluorescence time series observations for non-photochemical quenching and tidal variability reveals non-conservative phytoplankton variability in coastal waters. Limnol. Oceanogr. Methods. DOI: 10.1002/lom3.10325

Proctor, C. W., and C. S. Roesler. 2010. New insights on obtaining phytoplankton concentration and composition from in situ multispectral Chlorophyll fluorescence. Limnology and Oceanography: Methods **8:** 695-708.

Roesler, C. S. 2016. In Situ Chlorophyll Fluorescence Observations on NERACOOS Mooring A01: Revised Data Flagging and Changing Phenology. Boston: Massachusetts Water Resources Authority. Report 2016-15. 11 p. http://www.mwra.state.ma.us/harbor/enquad/pdf/2016-15.pdf

Roesler CS. 2020. Continuous observations of chlorophyll fluorescence and related parameters in Massachusetts Bay, 2005- 2019. Boston: Massachusetts Water Resources Authority. Report 2020-09. 27 p. http://www.mwra.state.ma.us/harbor/enquad/pdf/2020-09.pdf

Roesler, C. S. and A. H. Barnard, 2013. Optical proxy for phytoplankton biomass in the absence of photophysiology: Rethinking the absorption line height. Methods Oceanogr. 7: 79-94. Doi:10.1016/j.mio.2013.12.003 .

Roesler, C. S., J. Uitz, H. Claustre, E. Boss, X. Xing, E. Organelli, N. Briggs, A. Bricaud, C. Schmechtig, A. Poteau, F. D'Ortenzio, J. Ras, S. Drapeau, N. Haëntjens, and M. Barbieux, 2017a. Recommendations for obtaining unbiased chlorophyll estimates from in situ chlorophyll fluorometers: A global analysis of WET Labs ECO sensors. Limnol. Oceanogr. Methods, 15: 572–585. doi:10.1002/lom3.10185.

Roesler, C., V. Vellucci, J. Uitz, D. Antoine, H. Claustre., S. Drapeau, J. Ras. 2017b. Constructing in situ data set for phytoplankton functional type product validation. ASLO Aquatic Sciences Meeting, Honolulu, Hawaii, USA, 26 February-03 March 2017.

Thibodeau, P. S., C. S. Roesler, S. L. Drapeau, S. Prabhu Matondkar, J. I. Goes, and P. J. Werdell. 2014. Locating Noctiluca miliaris in the Arabian Sea: An optical proxy approach. Limnology and Oceanography **59:** 2042-2056.

Thomas, A.C., Pershing, A.J., Friedland, K.D., Nye, J.A., Mills, K.E., Alexander, M.A., Record, N.R., Weatherbee, R. and Henderson, M.E., 2017. Seasonal trends and phenology shifts in sea surface temperature on the North American northeastern continental shelf. *Elem Sci Anth*, 5, p.48. DOI: http://doi.org/10.1525/elementa.240

Thompson, M. (1998). Perspective: Do we really need detection limits? Analyst 123(2): 405-407.

Appendix. Data file formats.

Table A1. Format of the hourly observational data file for chlorophyll fluorescence data arrays, including those derived from FLNTU and FL3-WB sensors.

Column	ID	Value/Range	Comment
1	Year	2005-2020	
2	Month	1-12	
3	Day	0-31	
4	Hour	0-25	
5	Minute	0-60	
6	Second	0-60	
7	Date.Time	732607 - 738068	Matlab format
8	Raw Fchl	-1.63 – 162.56	Raw hourly mean
9	Flag_Offset	0, 1	Between deployments
10	Fchl_corr_offset		Corrected for offsets
11	Flag_Biofouling1	0, 1	Biofilm
12	Flag_Biofouling2	0, 1	Structural
13	Fchl_corr_biofouling	NaN	Values removed
14	Flag_NPQ	0, 1	NPQ
15	Fchl_corr_NPQ	-0.04 28.6	Values corrected (Carberry et al. 2019)
16	Flag_SVO	0, 1	Single value outlier
17	Fchl_corr_SVO	NaN	Values removed
18	Flag_MDL1	0, 1	< - Method detection level (MDL)
19	Flag_MDL2	0, 1	-MDL to 0
20	Flag_MDL3	0, 1	0 to +MDL
21	Fchl_corr	-0.04 to 29.47 /NaN	Cumulative removal/correction
22	Deployment	15 – 42	Deployment number
23	ECO-FLNTU S/N	001-9999	Sensor serial number, FLNTU

Table A2. Format of the hourly observational data file for Turbidity.

Column	ID	Value/Range	Comment
1	Year	2005-2020	
2	Month	1-12	
3	Day	0-31	
4	Hour	0-25	
5	Minute	0-60	
6	Second	0-60	
7	Date.Time	732607 - 737335	Matlab format
8	Raw Turbidity	-0.59 to 25.95	
9	Flag_Offset	0, 1	
10	Turb_corr_offset		Corrected for offsets
11	Flag_Biofouling1	0, 1	Biofilm
12	Flag_Biofouling2	0, 1	Structural
13	Turb_corr_biofouling	NaN	Values removed
14	Flag_SVO	0, 1	Single value outlier
15	Turb_corr_SVO	NaN	Values removed
16	Flag_MDL1	0, 1	< - Method detection level (MDL)
17	Flag_MDL2	0, 1	-MDL to 0
18	Flag_MDL3	0, 1	0 to +MDL
19	Turb_corr	-0.05 to 9.81 /NaN	Cumulative removal/correction
20	Deployment	15 - 42	Deployment number
21	ECO-FLNTU S/N	001-9999	Sensor serial number, FLNTU

Table A3. Format of the hourly observational data file for downwelling irradiance (ED) and upwelling radiance (LU).

Column	ID	Value/Range	Comment
1	Year	2005-2020	
2	Month	1-12	
3	Day	0-31	
4	Hour	0-25	
5	Minute	0-60	
6	Second	0-60	
7	Date.Time	732607 - 737335	Matlab format
8-14	Raw Ed(7)	-0.60 25.95	
15	Flag_Offset	0, 1	
16-22	Ed(7)_corr_offset		Corrected for spectral and intersensor offsets
23	Flag_Biofouling	0, 1	Biofouling
24-30	Ed(7)_corr_biofouling	NaN	Values removed
31	Flag_SVO	0, 1	Single value outlier
32	Flag_MDL1	0, 1	< - Method detection level (MDL)
33	Flag_MDL2	0, 1	-MDL to 0
34	Flag_MDL3	0, 1	0 to +MDL
35	Flag Cal	0, 1	Indicates multiplicative scaling
36-42	Ed(7)_final	NaN	Cumulative removal/correction
43	Deployment	15 – 42	Deployment number
44	OCI_507_SN	001-9999	OCI 507 sensor serial number

Table A4. List of submitted data arrays (.mat files) for chlorophyll fluorescence (from FLNTU sensor and each of the three channels of the F3WB sensor), turbidity, spectral irradiance, and central wavelengths of irradiance sensor.

Array Name	**Description**	**Units**	**Array size (row x columns)**	**Format**
H_Chl_42	hourly chlorophyll fluorescence, FLNTU	mg/m3	6074x23	Table A1
H_NTU_42	hourly turbidity	NTU	6074x21	Table A2
H_F1_42	Hourly chlorophyll fluorescence 435 nm excitation, F3WB	mg/m3	6074X23	Table A1
H_F2_42	Hourly chlorophyll fluorescence 470 nm excitation, F3WB	mg/m3	6074X23	Table A1
H_F3_42	Hourly chlorophyll fluorescence 532 nm excitation, F3WB	mg/m3	6074X23	Table A1
H_ED_42	Hourly spectral irradiance, 7 channels	μW/cm2/nm	6074x44	Table A3
H_ED_42_wave	Irradiance central wavelength	nm	7x1	n/a

Massachusetts Water Resources Authority
100 First Avenue • Boston, MA 02129
www.mwra.com
617-242-6000